scientific reports

OPEN

Target-specific peptides for BK virus agnoprotein identified through phage display screening: advancing antiviral therapeutics

Xiaofei Xing[1✉], Jingxian Han[2], Keke Wang[2], Fuyun Tian[1], CuiXia Jiang[1], Wei Liang[1], Lin Qi[1], Xin Yue[1], Yinhang Wen[1], Yuwei Hu[1] & Hui Qiao[1]

BK virus is implicated in polyomavirus-associated nephropathy (PVAN) and hemorrhagic cystitis, particularly in kidney transplant recipients, affecting the functionality of the transplanted kidney and posing a risk of graft loss. Despite these challenges, specific antiviral drugs targeting BK virus remain elusive. Agnoprotein, a small, positively charged protein encoded by the BK virus late gene, functions in the assembly, maturation, and release of the virus. Consequently, agnoprotein emerges as a promising target for potential anti-BK virus drugs. Utilizing phage display technology, we conducted screening to identify specific binding peptides against the agnoprotein. The primary objective of screening binding peptides is to utilize them to disrupt the virus's life cycle, impeding its replication and transmission, thereby achieving antiviral effects. In the current experimental study, a combination of phage 7 peptide libraries and 12 peptide libraries was employed for screening purposes. Following four rounds of screening, seven positive phages demonstrating the ability to bind Agnoprotein were successfully isolated. Following ELISA validation, it was observed that the optical density (OD) values for Agnoprotein binding of the seven positive clones significantly exceeded three times the value of the negative control (NC). Subsequent analysis identified one 7-peptide and six 12-peptides within the binding peptides. Moreover, OD values of dodecapeptide phage clones bound to agnoprotein were generally higher than those of heptapeptide phage clones. In conclusion, our study demonstrates the successful identification of specific binding peptides against agnoprotein, a crucial component in the BK virus life cycle.

Keywords BK virus, Kidney transplant, Agnoprotein, Phage display technology, Peptide drugs

Organ transplant surgery represents a sophisticated medical procedure that has undergone substantial advancements in recent decades. It holds the potential to save lives and enhance the quality of life for recipients. Notably, it serves as an efficacious treatment modality in various scenarios. For instance, heart transplantation can offer a lifeline to individuals with advanced heart disease unresponsive to alternative therapies, while kidney transplantation affords patients freedom from long-term dialysis dependence, facilitating a return to normalcy and the resumption of daily activities, including work. However, ensuring the long-term stability of transplanted organ function necessitates overcoming a series of challenges. Following organ transplantation, patients typically receive immunosuppressive therapy to prevent rejection of the transplanted organ by the immune system. However, these medications can compromise the patient's immune response, rendering them more susceptible to viral infections, including the BK virus. This virus is particularly impactful among kidney transplant recipients.

BK virus, a member of the Polyomavirus genus within the Polyomaviridae family, was initially isolated from a kidney transplant patient's urine[1,2]. This small, non-enveloped, circular double-stranded DNA virus possesses a genome size of approximately 5 kb[3]. Infection typically occurs during childhood, leading to latent persistence in various organs and tissues, particularly in epithelial cells of the kidneys and urogenital tract[4]. However, under conditions of immunosuppression, BK virus may undergo reactivation from latency[5], a phenomenon closely associated with the use of immunosuppressive agents post-transplantation[6,7]. The lack of an effective immune response can lead to polyomavirus-associated nephropathy in kidney transplant patients[8]. BK polyomavirus-

[1]Department of Clinical Laboratory, Zhengzhou No. 7 People's Hospital, 17 Jingnan 5th Road, Jingkai District, Zhengzhou, Henan, China. [2]Henan Key Laboratory of Cardiac Remodeling and Transplantation, Zhengzhou NO.7 People's Hospital, Zhengzhou, Henan, China. ✉email: xiiiiaofei@126.com

associated nephropathy occurs in 8% of kidney transplant recipients[9], with one study indicating that around 50% of these patients experience allograft loss within six months post-diagnosis, on average[10]. Cellular immunity plays a pivotal role in renal transplantation, with the most significant suppression occurring within the first year post-transplantation due to immunosuppressant usage. Viral replication frequently occurs during this period, resulting in the development of BK-associated nephropathy following a sustained exacerbation of BK viremia[5]. In severe cases, the function of the transplanted kidney may be compromised. Currently, there is a lack of specific antiviral drugs targeting BK virus, with control mainly achieved by adjusting the dosage of immunosuppressive agents, albeit at the risk of increased rejection[11,12]. Therefore, it is imperative to explore and develop targeted drugs against BK virus.

The gene coding region of BK virus encompasses the early coding region, responsible for large and small T-antigens, and the late coding region, which encodes the structural proteins VP1, VP2, and VP3, along with a regulatory protein known as agnoprotein[13,14]. Agnoprotein is uniquely expressed in three polyomaviruses: human polyomavirus JCV, BKV, and simian polyomavirus SV40, which share significant sequence homology[15,16]. Functionally, agnoprotein is a multifaceted player in various facets of the viral life cycle. Studies on SV40 and JCV have elucidated its involvement in viral DNA replication[17], nuclear export[18], transcriptional and post-transcriptional processes[19,20], maturation[21,22], protein stability[23,24], and localization. Additionally, it serves as a viral channel protein, augmenting cell membrane permeability and facilitating viral particle release[25,26]. Experimental evidence supports the notion that deletion or mutation of agnoprotein's coding region significantly diminishes viral gene expression and replication levels[22,27].

In BK virus, agnoprotein, a small basic protein consisting of 66 amino acids, is abundantly expressed in infected cells. Its amino acid sequence shares a high degree of similarity to SV40 and JCV agnoproteins, suggesting analogous functions. Several studies further corroborate this hypothesis. For instance, Myhre et al. identified a naturally occurring BK virus variant characterized by a deletion in the 5' end of the agnogene, resulting in the absence of agnoprotein expression upon transfection into Vero cells. Immunoelectron microscopy revealed the presence of virus-like particles within the transfected nuclei. The researchers then investigated the infectivity of these particles by lysing the transfected cells to release viral particles and inoculating the lysate into HUV-EC-C cells. However, no infectious progeny virus was detected in the cell culture supernatant. Subsequently, they reconstructed the variant with a complete coding sequence of agnoprotein, transfected Vero cells, and inoculated the supernatant into HUV-EC-C cells. Immunofluorescence staining demonstrated BK virus infection in the cell supernatant. Myhre et al.'s study concluded that BK virus's agnoprotein promotes the assembly, maturation, and release of infectious virions[28].

Panou conducted a similar study by mutating the agnogene of the clinical BK Dunlop strain and infecting RPTE cells with both mutant and wild-type BK virus. The results revealed a tenfold reduction in the proportion of mutant BK virus-infected cells releasing virus compared to the wild type. Further examination using electron microscopy at the single-cell level showed BK virus presence in both the nucleus and cytoplasm of wild-type BK virus-infected RPTE cells, whereas in cells infected with the mutant BK virus, virus presence was restricted to the nucleus. These findings indicate that agnoprotein is crucial for BK virion release from RPTE nuclei. Additionally, agnoprotein was found to interact with the binding protein α-SNAP, a crucial regulator of endoplasmic reticulum transport to the Golgi and vesicle transport. This interaction enables BK virus to transport virions from the nucleus to the cell exterior for release. Hence, the identification of a substance capable of binding to Agnoprotein could disrupt its interaction with α-SNAP, thereby inhibiting BK virus release from cells and impeding its diffusion and spread[29].

Peptides have emerged as compelling candidates for drug development owing to their distinctive biochemical and therapeutic properties, presenting advantages over small organic molecules. Notably, peptides exhibit enhanced tissue and organ penetration and demonstrate greater targeting specificity than their small organic counterparts[30,31]. In comparison to large molecular biologics, peptides offer benefits such as lower production costs, reduced immunogenicity, higher activity per unit mass, and enhanced storage stability[31,32]. Targeting viruses, peptides can be affixed to diverse carrier systems, including nanoparticles, liposomes, or phages[33–37], facilitating efficient tissue and cell penetration. In this experiment, the target protein Agnoprotein is mainly localized in the cytoplasm. Hence, the utilization of peptides facilitates a more straightforward penetration into cells, enabling effective binding to Agnoprotein. Peptide drugs have been widely used in the treatment of viral infections and other diseases. At present, more than 80 peptide drugs have received approval for marketing, with an additional 400–600 peptide drugs in various stages of preclinical trials[38,39].

Phage display technology is a potent tool for the development of novel peptide drugs[40]. Numerous peptide drugs derived from this technology have gained approval for marketing, demonstrating its efficacy. Among them, adalimumab is approved for the treatment of a variety of diseases, including rheumatoid arthritis, and juvenile idiopathic arthritis. Similarly, belimumab, discovered using antibody phage display technology, has received approval for managing systemic lupus erythematosus. Additionally, ecallantide (Kalbitor), a plasma potassium peptide inhibitor, is utilized in treating acute episodes of hereditary angioedema. Ecallantide's discovery stemmed from a phage display library constructed with the first Kunitz domain of a human lipoprotein-associated coagulation inhibitor, LACI-D1, as a scaffold[41]. The technique involves using phages as vectors to genetically engineer antibody fragments or peptides, preserving their spatial structure and biological activity[42,43], thus forming extensive peptide or antibody libraries. These libraries have a capacity exceeding 1.0×10^9, enabling efficient screening of specific targets such as proteins, protein receptors, tumor cells, and others[44]. Peptides offer several advantages over antibodies, prompting the utilization of phage peptide libraries as screening platforms in this study. When a large peptide library interacts with a specific target, the peptides displayed on the phage surface bind to the target. Subsequently, the bound phages are collected through elution, and the DNA within them is extracted to obtain sequence information of the interacting peptides. This sequence data enables the design and preparation of peptide drugs. Furthermore, medicinal chemistry techniques can be employed to

optimize and modify peptide sequences, enhancing their pharmacological properties such as biological stability, targeting, and efficacy.

In this study, a combination of the phage 7-peptide library and the 12-peptide library was screened using BK virus Agnoprotein as the target molecule, resulting in the identification of seven positive clones exhibiting robust binding capabilities. These peptides hold promise as prospective drugs targeting the BK virus. Drugs targeting agnoprotein may directly interfere with the processes of BK virus replication, assembly, maturation, and release from infected cells, thereby reducing viral load, relieving symptoms, and even blocking disease progression. This drug holds promise in significantly reducing the risk of patients developing BK virus-associated nephropathy, ultimately protecting long-term graft function, enhancing transplant success rates, and improving overall patient outcomes. Experimental Workflow of the Present Study can be found in Fig. 1.

Materials and methods
Expression and purification of agnoprotein
The genes encoding the external segment (Ser45-Ser66) and internal segment (Met1-Arg27) of Agnoprotein were expressed sequentially. Due to the protein's small size, we concatenated the external and internal segment genes three times using GGGS linkers and added two tags (SUMO and His). The target genes were inserted into the pET-28b vector. The constructed plasmid vector was then transformed into competent cells via heat shock. Transformed cells were cultured in LB liquid medium without antibiotics, and the mixture was plated on LB AGAR plates containing antibiotics, followed by overnight incubation at 37 °C. Single clones were selected from the overnight plates and cultured in LB liquid medium with appropriate antibiotics for 3–4 h.

Some cultures were induced with IPTG (final concentration = 1 mM) and grown at 37 °C/200 rpm for 4 h, while others were incubated overnight at 16 °C /200 rpm. After induction, bacterial cultures were collected by centrifugation to remove the supernatant. The pellet was resuspended in 1 ml 1× PBS buffer, and cell lysis was achieved by ultrasound. Following centrifugation at 10,000 rpm for 1 min, the supernatant labeled as "NPE" was collected, and excess supernatant was discarded. The pellet was resuspended in 100 μl 1× PBS containing 8 M
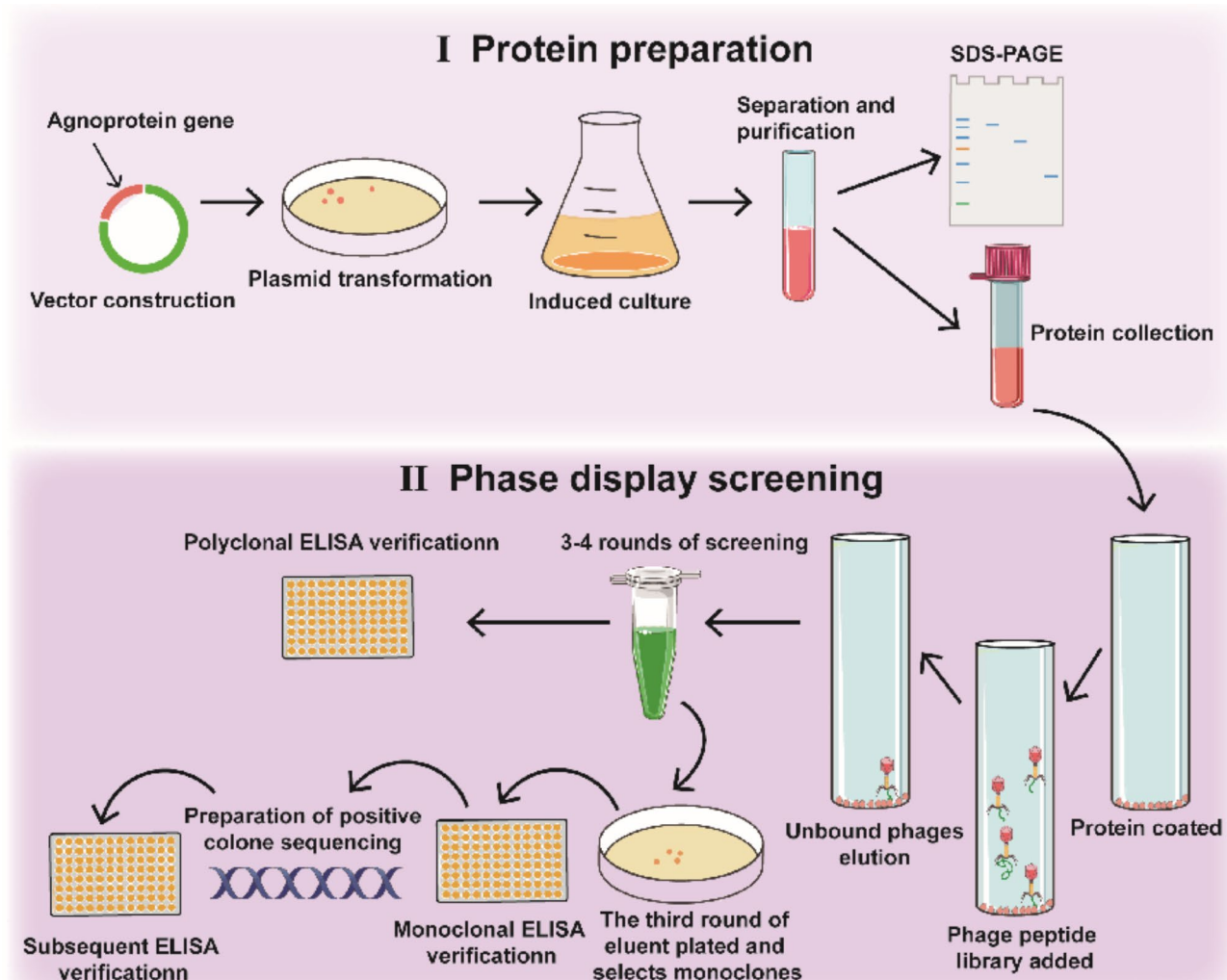

Fig. 1. Experimental Workflow of the Present Study. I, Expression and purification of Agnoprotein ; II, Flowchart of phage peptide library screening process.

urea, labeled as "DPE". Subsequently, 25 μl of 5× reducing loading buffer was added to the NPE and DPE samples and boiled for 10 min. SDS-PAGE was then performed on a 12% gel. Based on the results, conditions yielding the best expression were selected for large-scale culture to obtain more proteins.

The supernatant and inclusion body proteins were purified separately. For protein purification, cells were lysed with an appropriate amount of lysis buffer (PBS pH 7.5 + 10% glycerol + 1% PMSF), thoroughly mixed, and incubated for 20 min in an ultrasonic fragmentation device. The lysate was centrifuged at 12,000 rpm for 10 min to separate the supernatant (to be used for purifying the protein mixture) from the cell pellet. A certain amount of treated Ni resin was added to the supernatant mixture, and the resin was collected after incubation at 4 °C for 30 min. The flow-through solution (FT) solution was temporarily retained. Purification was then carried out, and samples were collected for SDS-PAGE. Following purification, the target protein was collected and dialyzed into the suitable buffer. Subsequently, protein concentrations were determined and subjected to SDS-PAGE analysis. Western blotting was used as a control method to detect the presence of the target proteins.

Phage Display Immunoaffinity selection (first round)

Immunotubes were coated with 1 mL of His-Agnoprotein (NPE) at a concentration of 50 μg/mL in buffered CBS and kept at 4 °C overnight. Subsequently, the immunotubes were rinsed three times with 5 mL PBST. An additional blocking step was performed using either 5% skim milk/PBST or 1% casein/PBST (5 mL each) for 1 h at 30 °C. Afterward, the immunotubes were washed once with 5 mL PBS. Following the blocking step, 1 mL of the phage library, containing 1×10^{12} pfu and comprising both the 7-peptide and 12-peptide libraries (purchased from NEB), was added to each tube and incubated for 2 h at 30 °C. The immunotubes were rinsed 4 to 6 times with 5 mL PBST. Phage elution was performed by adding 1 mL of Gly-HCl (pH = 2.2) to each tube, and the cells were incubated at room temperature for approximately 6–8 min with shaking. The solution was neutralized to a pH of 7.0–8.0 by adding 155 μL Tris-HCl (pH = 9.6). The eluted phage was diluted, *E. coli* TG1 in logarithmic phase was infected. The titer was determined by plate culturing.

Elution and amplification of phage

The eluted phages were aspirated and introduced into the logarithmic phase of *Escherichia coli* TG1 bacterial broth, followed by incubation at 37 °C for 4–6 h at 220 rpm. The culture medium was centrifuged (8000 rpm, 4 °C, 20 min), and the resulting supernatant was carefully transferred to a new centrifuge tube. Subsequently, a 1/4 volume of 5× PEG/NaCl solution was added, thoroughly mixed, and allowed to stand overnight at 4 °C. A second centrifugation (8000 rpm, 4 °C, 30 min) was performed, and the supernatant was discarded. The precipitate was then re-suspended in approximately 1 mL of PBS. Following a third centrifugation (8000 rpm, 10 min), the supernatant was transferred into a new centrifuge tube. The amplified phages were appropriately diluted, and used to infect the logarithmic phase TG1 *E. coli*. Titers were determined using the plaque assay method.

Immunoaffinity tube selection (second round to fourth round)

The amplified phage was employed for a second round of panning, repeating the same steps as described in 2.1 and 2.2. This process was iterated for a total of 4 rounds of panning. Immunotubes were coated with His-Agnoprotein (NPE) for the first and third rounds, and with His-Agnoprotein (DPE) for the second and fourth rounds.

Multi-clone phage ELISA detection

Immune plates were coated with 100 μL of His-Agnoprotein (NPE) and His-Agnoprotein (DPE) at a concentration of 4 μg/ml in buffered CBS. Control wells were coated with Nc-His (4 μg/ml, buffered CBS) and 100 μL PBS. The plates underwent three washes with 300 μL of PBST, and were then blocked with 300 μL 5% skim milk/PBST for 1 h at 30 °C, followed by 2–3 washes. The phages obtained after each round of amplification were diluted with PBS in 3-fold increments, starting from an initial concentration of 1×10^{12} pfu/ml. Subsequently, 100 μL of the diluted amplified phage was added to each well, incubated for 1 h at 30 °C, and washed 4–6 times with 300 μL PBST. A 100 μL solution of the secondary antibody (anti-phage M13) was added and incubated at 30 °C for 1 h, followed by washing with 300 μL PBST 4–6 times. Finally, 100 uL of the color development solution TMB was added and incubated for 3–8 min in the dark. The reaction was terminated by adding 50 μL of 2 M HCl, and the absorbance was measured using a microplate reader at 450 nm with a reference wavelength of 620 nm.

Monoclonal phage ELISA screening

The phages eluted from the third round were appropriately diluted and used to infect log-phase TG1 *E. coli*, spreading onto Petri dishes. On the next day, 192 monoclones were selected from the plates and transferred into deep-well plates for 6 h at 37 °C with shaking at 250 rpm. Afterward, the deep-well plates were centrifuged at 4000 rpm for 10–15 min, and the supernatant was collected for ELISA experiments. For ELISA, immune plates were coated with 100 μL of His-Agnoprotein (NPE) (4 μg/ml, buffered CBS), while control wells were coated with Nc-His (4 μg/ml, buffered CBS). The plates underwent three washes with 300 μL of PBST. Blocking was performed with 300 μL of 5% skim milk/PBST for 1 h at 30 °C, followed by 2–3 washes with 300 μL PBST. Subsequently, 100 μL of the phage supernatant was added to each well, and the plates were incubated for 1 h at 30 °C, followed by 4–6 washes with 300 μL PBST. A 100 μL solution of the secondary antibody (anti-M13) was added, incubated for 1 h at 30 °C, and washed 4–6 times with 300 μL PBST. Then, 100 μL of TMB was added in the dark for 3–8 min, and 50 μL of 2 M HCl was added to terminate the reaction. The microplate reader was used to measure absorbance at 450 nm with a reference wavelength of 620 nm. Positive clones were selected based on the criterion of AG > 3NC.

Identification and verification process for positive monoclonal clones

Positive clones obtained from monoclonal screening were analyzed using unidirectional reverse primers, specifically the 96 gIII primers (from the NEB kit): 5'-CCC TCA TAG TTA GCG TAA CG-3'. Positive clones were identified by excluding bimodular and repetitive sequences. The resulting DNA information was used to predict amino acid sequences, which were then aligned to check for duplications. Validation of the positive clones was performed through secondary ELISA. Immune plates were coated with 100 µL of His-Agnoprotein (NPE) and 100 µL of His-Agnoprotein (DPE) (4 µg/ml, buffered CBS). Control wells were coated with Nc-His (4 µg/ml, buffered CBS) and 100 µL PBS. The subsequent steps followed the protocol described in 2.6. After secondary ELISA verification, positive clones with AG > 3NC were selected.

Results

Protein expression and purification

Agnoprotein, being a transmembrane protein, led us to exclude its transmembrane region and instead focus on selecting its extracellular and intracellular segments for tandem expression. After concatenating the intracellular and extracellular gene segments, the ligation was performed using GGGS repeats three times. The target genes were then tagged with fusion tags SUMO and HIS. Subsequently, the target fragment was subcloned into the pET-28b vector using the NcoI/XhoI restriction sites. After vector construction, SnapGene was used for alignment to ensure the absence of mutations in the target gene. The plasmid was transformed into the expression strain for expression testing, and optimal expression conditions were identified for large-scale expression. Following expression, purification was conducted via Ni2 + affinity chromatography. The target protein was collected and dialyzed into the appropriate buffer, and its concentration of the protein was determined using the Bradford method. The concentration of NPE in the supernatant was measured at 0.25 mg/ml, while the concentration of inclusion body protein was 1.20 mg/ml. Notably, slight protein degradation occurred during the purification of the supernatant soluble protein NPE. To verify the results, SDS-PAGE was performed, with Western blot serving as a control. The SDS-PAGE results indicated successful expression of both fusion proteins. Due to the subsequent peptide library panning, we opted for proteins with small tags as raw materials for panning. Therefore, we chose to amplify and purify the His-Agnoprotein protein to finally obtain the target protein for panning peptide libraries. More details can be found in Figs. 2 and 3.

Selection results

In this experiment, four-well immune tubes were alternately coated with purified His-Agnoprotein (NEP) and His-Agnoprotein (DEP) proteins, in which DEP was added primarily to prevent nonspecific binding. The phage mixture library was then introduced for panning to identify phages binding specifically to His-Agnoprotein proteins. Phage titers were assessed after each round of screening, serving as an indicator of the enrichment level of phages specifically binding to His-Agnoprotein. The results revealed a significant increase in phage titer during the fourth round, suggesting that the phages had undergone enrichment due to specific binding to His-Agnoprotein. More details can be found in Table 1.
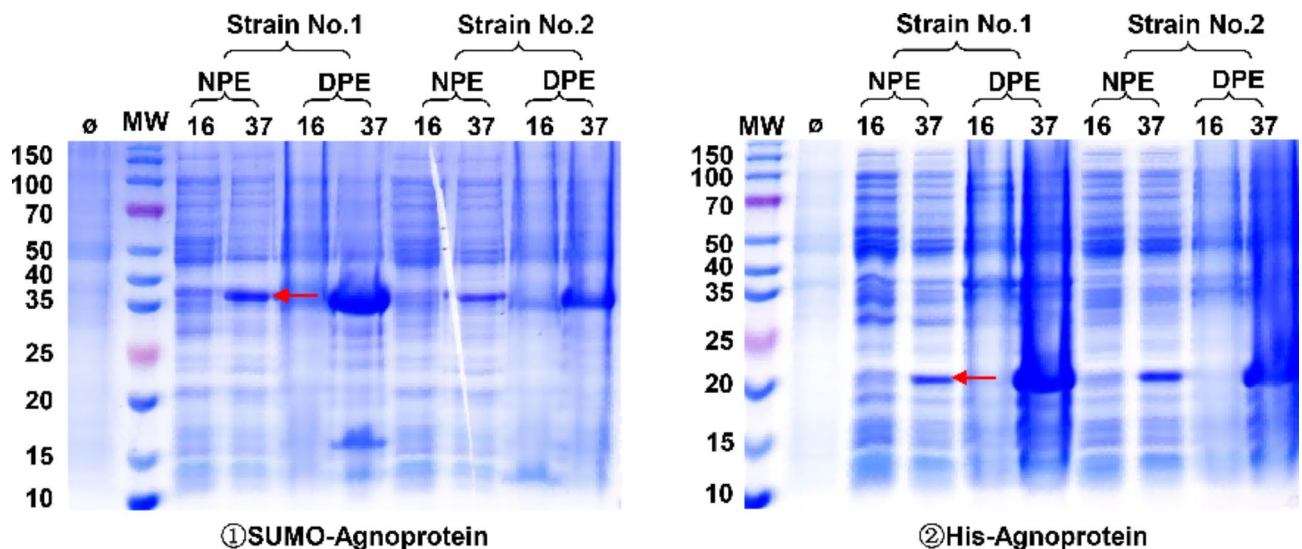

Fig. 2. Results of Agnoprotein Expression Test. ①Expression of SUMO-Agnoprotein protein by SDS-PAGE. ② Expression of His-Agnoprotein protein by SDS-PAGE. No.1, BL21(DE3) strain; No.2, T7E strain; NPE, Supernatant protein; DPE, Inclusion body protein; MW, Molecular weight; Ø, Uninduced strain (negative control); 16 °C、 37 °C, Induction expression temperatures; Expression test conditions, 1mM IPTG induction at 16 °C/16 h and 37 °C/4 h, respectively.
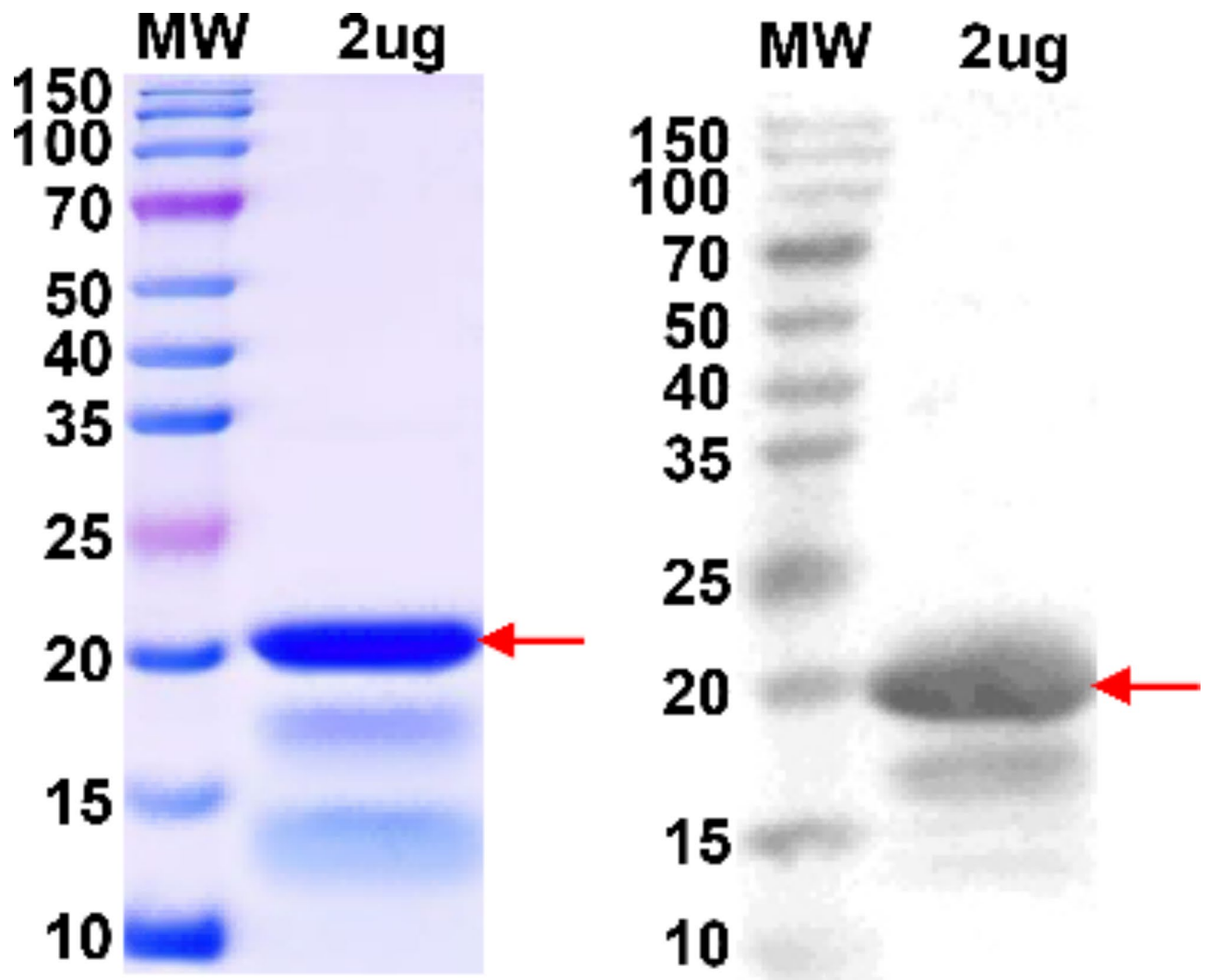
Fig. 3. Expression and purification results of His-Agnoprotein protein. Left, SDS-page result; Right, WB result. MW, Molecular weight; 2ug, Sample loading.

Rounds	Protein (µg/mL)	Input (pfu)	Output (pfu)
1	50/His-Agnoprotein (NPE)	1.0×10^{12}	2.2×10^{7}
2	50/His-Agnoprotein (DPE)	1.0×10^{12}	4.3×10^{7}
3	50/His-Agnoprotein (NPE)	1.0×10^{12}	4.0×10^{6}
4	50/His-Agnoprotein (DPE)	1.0×10^{12}	4.4×10^{7}

Table 1. Selection results. NPE, Supernatant Protein; DPE, Inclusion Body Protein.

ELISA results for polyclonal phages

Immune plates were coated with antigen His-Agnoprotein (NPE) and antigen His-Agnoprotein (DPE). Phages from each round of amplification were introduced in 3-fold dilution increments. Following this, a series of steps was conducted: incubation, washing, addition of secondary antibodies, color development, and measurement using a microplate reader. Upon analyzing the results, a clear trend emerged: as the phage concentration decreased gradually, the measured OD values post-binding to Ag1 and Ag2 also decreased incrementally. However, intriguingly, the OD value of phage binding to Ag2 (DPE) surpassed that of Ag1 (NPE). This observation may be attributed to the higher concentration of DPE compared to NPE, allowing for a greater number of phages to bind. Among the four rounds, the third round exhibited the highest positivity rate, with generally elevated OD values. Hence, the decision was made to focus on monoclonal clones sourced from the eluted phages of the third round for subsequent screening. More details can be found in Fig. 4 .
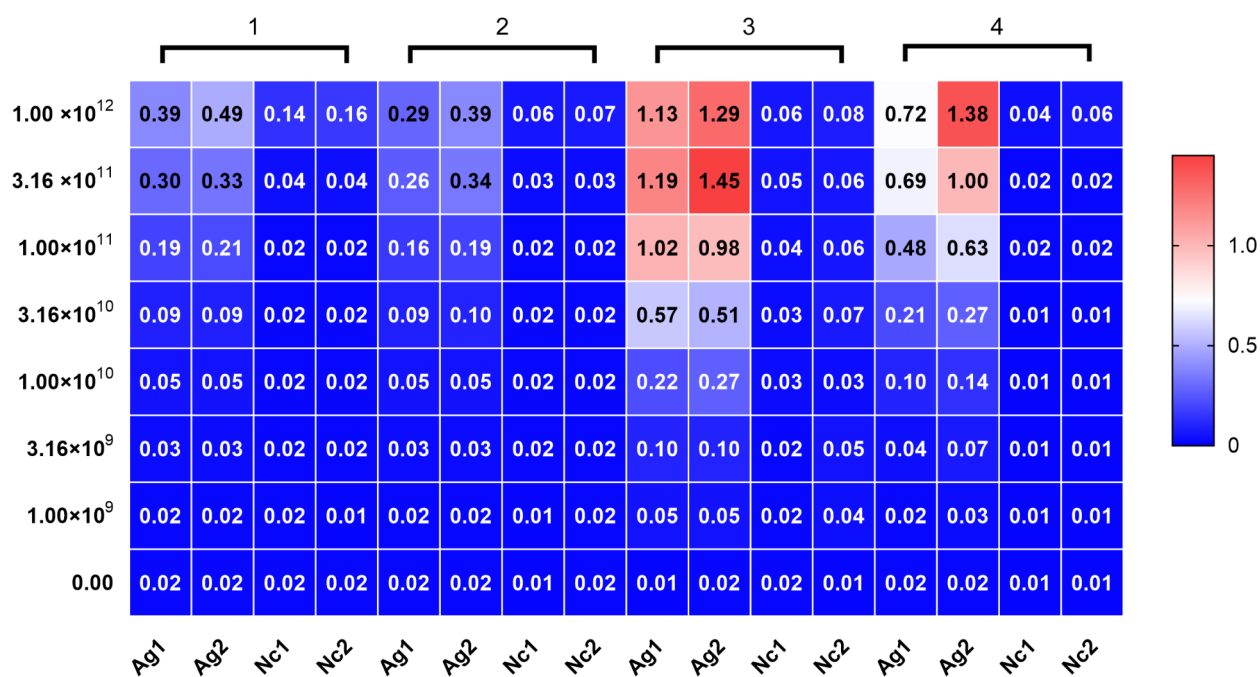
Fig. 4. ELISA Results of Polyclonal Phage. 1, 2, 3, 4, Four rounds of phage screening; 0.00, 1.00×10^9, 3.16×10^9, 1.00×10^{10}, 3.16×10^{10}, 1.00×10^{11}, 3.16×10^{11}, 1.00×10^{12}, The concentration of phages; Ag1, His-Agnoprotein (NPE); Ag2, His-Agnoprotein (DPE); Nc1,Nc-His; Nc2,PBS; Data in each cell, Absorbance value (OD value).

Single-clone phage ELISA screening

The phages eluted from the third round were appropriately diluted and used to infect logarithmic phase *E. coli* TG1 for plating. On the next day, 192 monoclones were selected from the plates, cultured, centrifuged and the supernatant was used for ELISA experiments. There are notable variations in experimental design between monoclonal and polyclonal phage ELISA methods. In polyclonal ELISA, it is customary to coat several different antigens simultaneously. In our study, we coated two antigens, His-Agnoprotein (NPE) and His-Agnoprotein (DPE), simultaneously. This approach enables the concurrent examination of multiple antigen bindings within the same assay. Conversely, monoclonal ELISA focuses on a single antigen, in this case, His-Agnoprotein (NPE), to ensure the specificity and accuracy of test results. In polyclonal ELISA, the phage supernatant harbors numerous monoclonal clones, potentially resulting in multiple phages recognizing different epitopes, thereby increasing the likelihood of cross-reactions. However, monoclonal phage ELISA employs supernatant derived from a specific single clone, containing only one phage, thus eliminating cross-reactions. Consequently, monoclonal phage ELISA typically exhibits higher specificity and consistency. Following monoclonal phage ELISA, nine clones exhibiting higher OD values were selected and sequenced. After excluding double peak and repetitive sequences, we identified seven distinct sequences. More details can be found in Figs. 5 and 6 .

Results of the secondary ELISA detection

The seven positive clones obtained were subjected to verification through secondary ELISA. The OD values observed for these seven phage clones, in conjunction with Ag1 (NPE) and Ag2 (DPE), markedly exceeded those of the control group (NC). Specifically, their values surpassed three times the OD value of the control group. This indicates that these clones demonstrate substantial binding affinities for both Ag1 and Ag2. More details can be found in Table 2.

Characterization and binding efficiency analysis of positive clones

The secondary verification confirmed the positivity of these 7 distinct clones. Subsequent analysis and alignment revealed the presence of one heptapeptide sequence and six dodecapeptide sequences across these clones. Interestingly, the OD values observed for the dodecapeptide phage clones binding to agnoprotein generally surpassed those of the heptapeptide phage clones. This observation suggests that phage clones harboring longer peptides exhibit a more robust binding capacity. This phenomenon may be explained by the fact that the longer peptide provides more binding sites and thus increases the possibility of binding to the agnoprotein, resulting in higher OD values. More details can be found in Table 3.
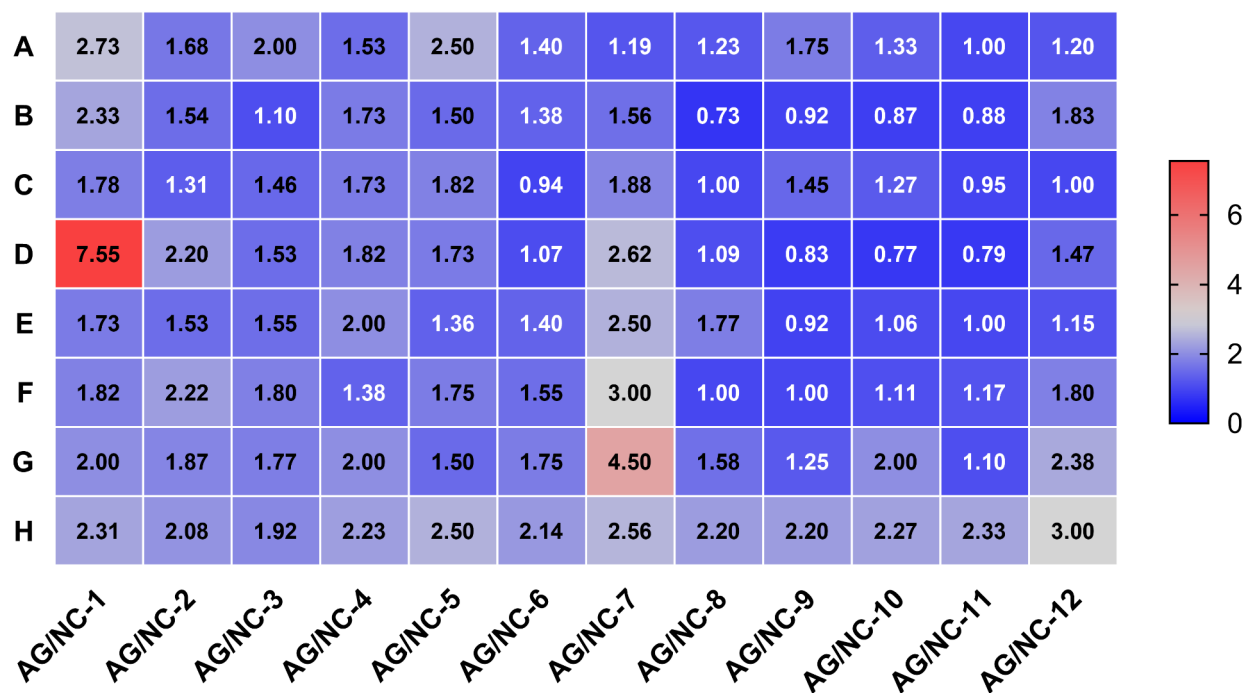
Fig. 5. ELISA Results of R3P1 Monoclonal Phage. R3, Monoclonal phage in the third round of screening; P1, The first culture plate; AG, His-Agnoprotein (NPE) ; NC, NC-His; Data in each cell, OD value of AG/OD value of NC; Positive clones were selected based on the criterion of AG > 3NC.

Discussion

Viruses employ an array of strategies not only to modulate their hosts but also to manipulate the surrounding cellular environment, ensuring a successful life cycle and efficient reproduction of their progeny. One such mechanism involves the secretion of specific proteins to alter the nearby cellular milieu, creating conditions favorable for the next round of viral replication[45]. In this intricate process, the agnoprotein of the BK virus emerges as a pivotal regulatory factor. Encoded by the late gene coding region, agnoprotein is a small, phosphorylated protein that forms stable dimers and oligomers both in vivo and in vitro. Although primarily localized in the cytoplasm, it significantly accumulates in the perinuclear region of infected cells[46–49]. Functionally, agnoprotein of the BK virus plays a facilitating role in various aspects of the virus life cycle, including assembly, maturation, and release. This implies its involvement in key steps such as viral particle formation, assembly of envelope proteins, and virus release from infected cells. Similarly, the agnoproteins of SV40 and JCV viruses are implicated in vital life cycle processes like replication and transcription. Given the high homology between the agnoproteins of BK virus and those of SV40 and JCV[15,16], it is reasonable to infer that BK virus agnoproteins may share similar functions and mechanisms of action. In summary, targeting agnoprotein offers a promising approach for drug design aimed at disrupting its function and interactions. Subsequent drug screening and optimization research based on this target molecule could open new therapeutic avenues for the treatment of BK virus infection, potentially offering patients more effective treatment options.

Recognizing the pivotal role of agnoprotein, we targeted it for drug identification through screenings using a phage peptide library. The concept of phage display was first described in 1985 for presenting short peptide sequences[50], and gained recognition with the submission of the first patent in 1991 (US5223409). Since then, phage display has emerged as a reliable method for generating peptides with potential therapeutic or diagnostic utility[51]. This technology has significantly contributed to the development of peptide drugs targeting various diseases, including hereditary angioedema, immune thrombocytopenic purpura, rheumatoid arthritis, and uveitis[38–40]. To enhance the efficiency of screening positive phage peptides targeting agnoprotein, we employed a mixed library comprising both phage 7-peptide and 12-peptide libraries. This approach led to the identification of seven phage peptides exhibiting the most robust binding capacity. Remarkably, six of these positive phage clones featured a twelve-peptide length, while only one clone had a heptapeptide length. This outcome highlights the superiority of dodecapeptide phages in binding to agnoprotein, likely attributable to the longer peptide offering more binding sites and thereby enhancing the probability of binding to agnoprotein.

Nevertheless, our study has several limitations that warrant consideration. Firstly, the expression of agnoprotein is not in its full-length form but consists of intracellular and extracellular segments, lacking the transmembrane region. This may result in the omission of peptides that interact with the transmembrane region, potentially affecting the accuracy of our findings. Additionally, during the screening process, non-specific reactions may occur, leading to false positive results. To mitigate this, we implemented alternate screenings of
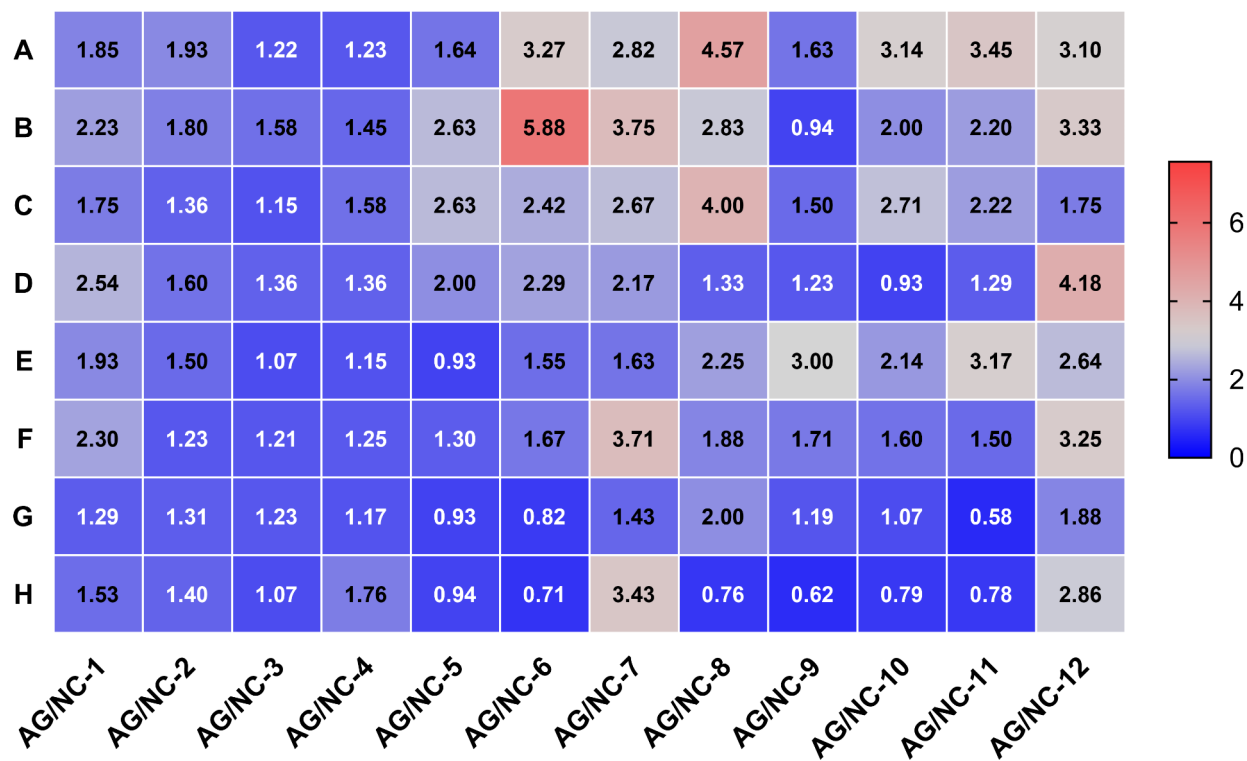
Fig. 6. ELISA Results of R3P2 Monoclonal Phage. R3, Monoclonal phage in the third round of screening; P2, The second culture plate; AG, His-Agnoprotein (NPE) ; NC, NC-His; Data in each cell, OD value of AG/OD value of NC; Positive clones were selected based on the criterion of AG > 3NC.

Clone	Ag1	Ag2	Nc1	Nc2
R3P1-D1	0.59	0.90	0.02	0.02
R3P1-G7	0.24	0.41	0.02	0.02
R3P2-B7	0.29	0.60	0.02	0.03
R3P2-A8	0.82	1.36	0.02	0.03
R3P2-C8	0.32	0.68	0.03	0.04
R3P2-A11	0.73	1.21	0.03	0.04
R3P2-D12	1.23	1.94	0.04	0.06

Table 2. Results of the secondary ELISA detection. Ag1, His-Agnoprotein (NPE) ; Ag2, His-Agnoprotein (DPE) ; Nc1, Nc-His ; Nc2, PBS.

Clone	Gene sequence	Peptide sequence
R3P1-D1	ACGGTTATTAAGCTTAAGCCGGATGCTATTCCTTCG	TVIKLKPDAIPS
R3P1-G7	GTGGCGTCTGGGACTGTGTTTGGTGATGCGCCGAGT	VASGTVFGDAPS
R3P2-B7	TTTGCGTTGACGAATGTGAAT	FALTNVN
R3P2-A8	GCTTTTTGGCAGCCGCAGTTGAATCCGAGGTGGGCG	AFWQPQLNPRWA
R3P2-C8	GGTGCGTATCATCCGGTGTCTCGGGCGCTGTCTACG	GAYHPVSRALST
R3P2-A11	CAGACGATGAATACTTGGTATCGGACGTTTAATATG	QTMNTWYRTFNM
R3P2-D12	CAGGGTTTTTTGCCTCCGTATCAGAATGATTTTCCG	QGFLPPYQNDFP

Table 3. Analysis results of 7 clones.

superalbumin and inclusion body proteins. We used His labeled Agnoprotein constructs in our experiments, which may be different from the natural structure, and thus have a certain impact on the physiological relevance of screening peptides. In view of this limitation, we will further verify the function of the screening peptides in the future, and plan to use unlabeled natural conformational proteins for experiments in the future to improve the accuracy and reliability of the study.

In conclusion, this study marks the first instance of utilizing a mixed phage peptide library to screen for binding peptide targeting the agnoprotein of the BK virus. Beyond their potential as targeted peptide drugs against BK virus infection, these screened binding peptides hold significant promise in other applications. Firstly, they can serve as carriers for precise drug delivery to virus-infected cells or tissues, enhancing drug bioavailability and therapeutic efficacy. Additionally, by binding to the unique agnoprotein of the BK virus, these peptides can aid in the development of diagnostic reagents with high sensitivity and specificity, offering more accurate clinical diagnosis. Moreover, incorporating these binding peptides into therapeutic vaccines can induce specific immune responses in the immune system, aiding in disease prevention. Hence, these binding peptides provide both theoretical and experimental groundwork for realizing these potential applications in the future.

Data availability

The data generated and analyzed during this study are available from the corresponding author upon reasonable request. Researchers interested in accessing the data should contact Hui Qiao at Email: 15237182182@139.com.

References
1. Gardner, S. D., Field, A. M., Coleman, D. V. & Hulme, B. New human papovavirus (B.K.) isolated from urine after renal transplantation. *Lancet* **297** (7712), 1253–1257 (1971).
2. Moens, U. et al. ICTV Virus Taxonomy Profile: Polyomaviridae. *J. Gen. Virol.* **98** (6), 1159–1160 (2017).
3. Blackard, J. T., Davies, S. M. & Laskin, B. L. BK Polyomavirus diversity-why viral variation matters. *Rev. Med. Virol.* **30** (4), e2102 (2020).
4. Borriello, M. et al. BK Virus infection and BK-Virus-Associated Nephropathy in Renal Transplant recipients. *Genes* **13** (7), 1290 (2022).
5. Kant, S., Dasgupta, A., Bagnasco, S. & Brennan, D. C. BK Virus Nephropathy in kidney transplantation: a state-of-the-art review. *Viruses* **14** (8), 1616 (2022).
6. Binet, I. et al. Polyomavirus disease under new immunosuppressive drugs: a cause of renal graft dysfunction and graft loss. *Transplantation* **67** (6), 918–922 (1999).
7. Comoli, P., Binggeli, S., Ginevri, F. & Hirsch, H. H. Polyomavirus-associated nephropathy: update on BK virus-specific immunity. *Transpl. Infect. Dis.* **8** (2), 86–94 (2006).
8. Balba, G. P., Javaid, B. & Timpone, J. G. BK Polyomavirus infection in the renal transplant recipient. *Infect. Dis. Clin. North. Am.* **27** (2), 271–283 (2013).
9. Hirsch, H. H. et al. Prospective study of polyomavirus type BK replication and nephropathy in renal-transplant recipients. *N Engl. J. Med.* **347** (7), 488–496 (2002).
10. Nickeleit, V. et al. BK-virus nephropathy in renal transplants-tubular necrosis, MHC-class II expression and rejection in a puzzling game. *Nephrol. Dial Transpl.* **15** (3), 324–332 (2000).
11. Helle, F. et al. Biology of the BKPyV: an update. *Viruses* **9** (11), 327 (2017).
12. Kuypers, D. R. J. Management of polyomavirus-associated nephropathy in renal transplant recipients. *Nat. Rev. Nephrol.* **8** (7), 390–402 (2012).
13. Buck, C. B. Exposing the Molecular Machinery of BK Polyomavirus. *Structure* **24** (4), 495 (2016).
14. Ehlers, B. & Moens, U. Genome analysis of non-human primate polyomaviruses. *Infect. Genet. Evol.* **26**, 283–294 (2014).
15. White, M. K. & Khalili, K. Expression of JC virus regulatory proteins in human cancer: potential mechanisms for tumourigenesis. *Eur. J. Cancer*. **41** (16), 2537–2548 (2005).
16. Safak, M. et al. Interaction of JC virus agno protein with T antigen modulates transcription and replication of the viral genome in glial cells. *J. Virol.* **75** (3), 1476–1486 (2001).
17. Saribas, A. S., White, M. K. & Safak, M. JC virus agnoprotein enhances large T antigen binding to the origin of viral DNA replication: evidence for its involvement in viral DNA replication. *Virology* **433** (1), 12–26 (2012).
18. Okada, Y. et al. Dissociation of heterochromatin protein 1 from lamin B receptor induced by human polyomavirus agnoprotein: role in nuclear egress of viral particles. *EMBO Rep.* **6** (5), 452–457 (2005).
19. Safak, M., Sadowska, B., Barrucco, R. & Khalili, K. Functional interaction between JC virus late regulatory agnoprotein and cellular Y-box binding transcription factor, YB-1. *J. Virol.* **76** (8), 3828–3838 (2002).
20. Saribas, A. S. et al. Essential roles of Leu/Ile/Phe-rich domain of JC virus agnoprotein in dimer/oligomer formation, protein stability and splicing of viral transcripts. *Virology* **443** (1), 161–176 (2013).
21. Hou-Jong, M. H., Larsen, S. H. & Roman, A. Role of the agnoprotein in regulation of simian virus 40 replication and maturation pathways. *J. Virol.* **61** (3), 937–939 (1987).
22. Ellis, L. C., Norton, E., Dang, X. & Koralnik, I. J. Agnogene deletion in a novel pathogenic JC virus isolate impairs VP1 expression and virion production. Fujinami RS, ed. *PLOS One.* ;8(11):e80840. (2013).
23. Margolskee, R. F. & Nathans, D. Suppression of a VP1 mutant of simian virus 40 by missense mutations in serine codons of the viral agnogene. *J. Virol.* **48** (2), 405–409 (1983).
24. Carswell, S. & Alwine, J. C. Simian virus 40 agnoprotein facilitates perinuclear-nuclear localization of VP1, the major capsid protein. *J. Virol.* **60** (3), 1055–1061 (1986).
25. Suzuki, T. et al. The human polyoma JC virus agnoprotein acts as a viroporin. Imperiale MJ, ed. *PLOS Pathog.* ;6(3):e1000801. (2010).
26. Suzuki, T. et al. Viroporin activity of the JC Polyomavirus is regulated by interactions with the adaptor protein complex 3. *Proc. Natl. Acad. Sci. U S A*. **110** (46), 18668–18673 (2013).
27. Sariyer, I. K., Saribas, A. S., White, M. K. & Safak, M. Infection by agnoprotein-negative mutants of polyomavirus JC and SV40 results in the release of virions that are mostly deficient in DNA content. *Virol. J.* **8** (1), 255 (2011).
28. Myhre, M. R., Olsen, G. H., Gosert, R., Hirsch, H. H. & Rinaldo, C. H. Clinical polyomavirus BK variants with agnogene deletion are non-functional but rescued by trans-complementation. *Virology* **398** (1), 12–20 (2010).
29. Panou, M. M. et al. Agnoprotein is an essential egress factor during BK Polyomavirus infection. *Int. J. Mol. Sci.* **19** (3), 902 (2018).

30. Lee, A. C. L., Harris, J. L., Khanna, K. K. & Hong, J. H. A Comprehensive Review on current advances in peptide Drug Development and Design. *Int. J. Mol. Sci.* **20** (10), 2383 (2019).
31. Ladner, R. C., Sato, A. K., Gorzelany, J. & De Souza, M. Phage display-derived peptides as therapeutic alternatives to antibodies. *Drug Discovery Today*. **9** (12), 525–529 (2004).
32. Molek, P., Strukelj, B. & Bratkovic, T. Peptide phage display as a Tool for Drug Discovery: Targeting membrane receptors. *Molecules* **16** (1), 857–887 (2011).
33. Nilsson, F., Tarli, L., Viti, F. & Neri, D. The use of phage display for the development of tumour targeting agents. *Adv. Drug Delivery Rev.* **43** (2–3), 165–196 (2000).
34. Yoo, M. K. et al. Targeted delivery of chitosan nanoparticles to Peyer's patch using M cell-homing peptide selected by phage display technique. *Biomaterials* **31** (30), 7738–7747 (2010).
35. Lee, T. Y., Lin, C. T., Kuo, S. Y., Chang, D. K. & Wu, H. C. Peptide-mediated targeting to tumor blood vessels of lung cancer for drug delivery. *Cancer Res.* **67** (22), 10958–10965 (2007).
36. Li, Z., Zhang, J., Zhao, R., Xu, Y. & Gu, J. Preparation of peptide-targeted phagemid particles using a protein III-modified helper phage. *BioTechniques* **39** (4), 493–497 (2005).
37. Larocca, D. et al. Evolving phage vectors for cell targeted gene delivery. *Curr. Pharm. Biotechnol.* **3** (1), 45–57 (2002).
38. Lau, J. L. & Dunn, M. K. Therapeutic peptides: historical perspectives, current development trends, and future directions. *Bioorg. Med. Chem.* **26** (10), 2700–2707 (2018).
39. Özçelik, C. E. et al. Synergistic screening of peptide-based Biotechnological Drug candidates for neurodegenerative diseases using yeast Display and Phage Display. *ACS Chem. Neurosci.* **14** (19), 3609–3621 (2023).
40. Omidfar, K. & Daneshpour, M. Advances in phage display technology for drug discovery. *Expert Opin. Drug Discovery*. **10** (6), 651–669 (2015).
41. Markland, W., Ley, A. C. & Ladner, R. C. Iterative optimization of high-affinity protease inhibitors using phage display. 2. Plasma kallikrein and thrombin. *Biochemistry* **35** (24), 8058–8067 (1996).
42. Liu, P., Han, L., Wang, F., Petrenko, V. A. & Liu, A. Gold nanoprobe functionalized with specific fusion protein selection from phage display and its application in rapid, selective and sensitive colorimetric biosensing of Staphylococcus aureus. *Biosens. Bioelectron.* **82**, 195–203 (2016).
43. Rahbarnia, L. et al. Evolution of phage display technology: from discovery to application. *J. Drug Target.* **25** (3), 216–224 (2017).
44. Plessers, S., Van Deuren, V., Lavigne, R. & Robben, J. High-throughput sequencing of phage display libraries reveals Parasitic Enrichment of Indel mutants caused by amplification Bias. *Int. J. Mol. Sci.* **22** (11), 5513 (2021).
45. Saribas, A. S., Coric, P., Bouaziz, S. & Safak, M. Expression of novel proteins by polyomaviruses and recent advances in the structural and functional features of agnoprotein of JC virus, BK virus, and simian virus 40. *J. Cell. Physiol.* **234** (6), 8295–8315 (2019).
46. Frisque, R. J., Bream, G. L. & Cannella, M. T. Human polyomavirus JC virus genome. *J. Virol.* **51** (2), 458–469 (1984).
47. Saribas, A. S. et al. Emerging from the unknown: structural and functional features of Agnoprotein of Polyomaviruses. *J. Cell. Physiol.* **231** (10), 2115–2127 (2016).
48. Rinaldo, C. H. & Hirsch, H. H. Antivirals for the treatment of polyomavirus BK replication. *Expert Rev. Anti-Infect Ther.* **5** (1), 105–115 (2007).
49. Nomura, S., Khoury, G. & Jay, G. Subcellular localization of the simian virus 40 agnoprotein. *J. Virol.* **45** (1), 428–433 (1983).
50. Smith, G. P. Filamentous fusion phage: novel expression vectors that display cloned antigens on the virion surface. *Science* **228** (4705), 1315–1317 (1985).
51. Brown, K. C. Peptidic tumor targeting agents: the road from phage display peptide selections to clinical applications. *Curr. Pharm. Des.* **16** (9), 1040–1054 (2010).

Acknowledgements

Author contributions
X.X wrote the main manuscript text and Fig. 1 and J.H and K.W and F.T prepared Figs. 2 and 3 and W.L and L.Q and C.J prepared Fig. 4 and X.Y and Y.W and W.H and H.Q prepared Figs. 5 and 6.

Declarations

Competing interests
The authors declare no competing interests.

Additional information
Correspondence and requests for materials should be addressed to X.X.

Reprints and permissions information is available at www.nature.com/reprints.

Publisher's note Springer Nature remains neutral with regard to jurisdictional claims in published maps and institutional affiliations.